

PAPER • OPEN ACCESS

EUV spectral shape variation of tungsten unresolved transition arrays in electron temperature range of 2–4 keV observed in the Large Helical Device

To cite this article: T Oishi *et al* 2023 *J. Phys.: Conf. Ser.* **2439** 012005

View the [article online](#) for updates and enhancements.

You may also like

- [Characteristics of x-ray emission from optically thin high-Z plasmas in the soft x-ray region](#)
Hayato Ohashi, Takeshi Higashiguchi, Yuhei Suzuki *et al.*
- [EUV spectroscopy of highly charged high Z ions in the Large Helical Device plasmas](#)
C Suzuki, F Koike, I Murakami *et al.*
- [XUV spectral analysis of ns- and ps-laser produced platinum plasmas](#)
Tao Wu, Takeshi Higashiguchi, Bowen Li *et al.*



244th Electrochemical Society Meeting

October 8 – 12, 2023 • Gothenburg, Sweden

50 symposia in electrochemistry & solid state science

Abstract submission deadline:
April 7, 2023

Read the call for papers &
submit your abstract!

EUV spectral shape variation of tungsten unresolved transition arrays in electron temperature range of 2–4 keV observed in the Large Helical Device

T Oishi^{1,2}, S Morita^{1,2}, I Murakami^{1,2}, D Kato^{1,3}, H A Sakaue¹, Y Kawamoto¹, T Kawate^{1,2} and M Goto^{1,2}

¹ National Institute for Fusion Science, National Institutes of Natural Sciences, 322-6, Oroshi-cho, Toki, Gifu 509-5292, Japan

² Department of Fusion Science, The Graduate University for Advanced Studies, SOKENDAI, 322-6, Oroshi-cho, Toki, Gifu 509-5292, Japan

³ Interdisciplinary Graduate School of Engineering and Sciences, Kyushu University, Kasuga, Fukuoka 816-8580, Japan

oishi@nifs.ac.jp

Abstract. Spectroscopic studies of emissions released from tungsten ions combined with a pellet injection technique have been conducted in the Large Helical Device. The tungsten Unresolved Transition Array (UTA) spectrum was observed in the wavelength ranges of extreme ultraviolet (EUV) 6–60 Å and 130–340 Å, and the electron temperature dependence of the UTA spectral shape was investigated in the electron temperature region < 4.3 keV. The UTAs of W^{24+} – W^{33+} at 20–33 Å, W^{37+} – W^{42+} at 45–47 Å, W^{27+} – W^{29+} at 48–55 Å, and W^{7+} – W^{27+} at 170–210 Å were observed. Unidentified UTAs were also found at 230–270 Å and 280–320 Å. As the electron temperature increased further above 4 keV, the W^{37+} – W^{42+} UTA at 45–47 Å was maintained, while the other UTAs became less intense.

1. Introduction

Tungsten is a candidate material for plasma-facing components in ITER and future fusion reactors because of its high melting point, low sputtering yield, and low tritium retention [1]. On the other hand, there is a concern that tungsten ions with a large atomic number of $Z = 74$ will cause large energy loss by radiation and ionization when the plasma is contaminated by tungsten impurity. In high- Z ions such as tungsten, a pseudo-continuous emission spectrum that cannot be resolved into single spectral lines, called the Unresolved Transition Array (UTA), is observed [2]. Therefore, it is necessary to accumulate spectroscopic data of UTA spectra for quantitative analysis on tungsten impurity behavior in high temperature plasmas.

2. Tungsten pellet injection experiment in LHD

Spectroscopic studies for tungsten emissions have been intensively conducted in the Large Helical Device (LHD), which is a superconducting plasma confinement device with a heliotron magnetic configuration [3]. Tungsten ions are distributed in the LHD plasma by injecting a pellet consisting of a small piece of tungsten metal wire enclosed by a carbon tube. Emission lines of tungsten ions from



W^0 – W^{46+} have been observed via extreme ultraviolet (EUV), vacuum ultraviolet (VUV), and visible spectroscopy [4–6]. In this paper, the tungsten UTA spectra observed using two flat-field EUV spectrometers in the wavelength ranges 6–60 Å and 130–340 Å are presented. Figure 1 shows a waveform of a tungsten pellet injection experiment in a hydrogen discharge with the position of the magnetic axis at 3.6 m and the toroidal magnetic field of 2.75 T in the counter-clockwise direction. The plasma was initiated by electron cyclotron heating (ECH) and sustained by negative and positive ion source-based hydrogen neutral beam injection heating (n-NBI and p-NBI, respectively) as shown in Fig. 1(a). A tungsten pellet was injected at $t = 4.05$ s. The central electron temperature, T_{e0} , once decreased from 3 keV to 2 keV, and then started to increase by superposition of ECH from $t = 4.2$ s as shown in Fig. 1(b). The central electron density, n_{e0} , and the total radiation power, P_{rad} , increased rapidly with tungsten injection as shown in Figs. 1(c) and (d), respectively. The high value of P_{rad} is an indicator that the tungsten ions remain in the plasma and serve as radiation sources. However, P_{rad} quickly turned to decrease and returned to the level before tungsten injection after $t=5.0$ s. This suggests that the injected tungsten is almost completely exhausted and there is no longer a strong radiation source. Therefore, this paper presents tungsten emission spectra from 4.0 s to 5.0 s. On the other hand, we have observed some cases that the injected tungsten ions remain in the plasma for a long time, which is more pronounced at higher electron densities. In these cases, characteristic tungsten spectra are observed even during the latter half of the discharge with the low electron temperature below 1 keV, and the spectral shape is summarized in Ref. [4].

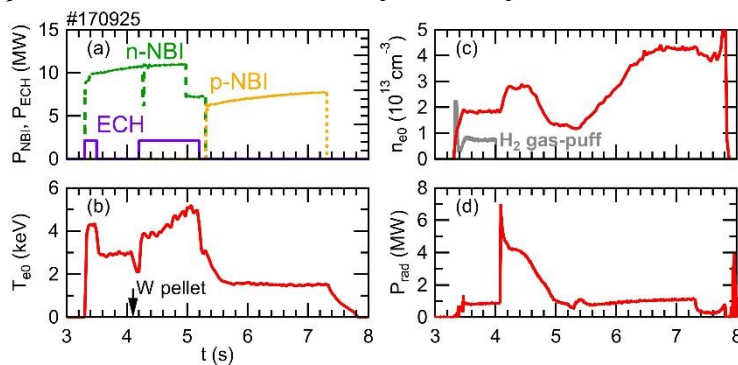


Figure 1. Waveform of tungsten pellet injection experiment in LHD. (a) Heating power of NBI and ECH, P_{NBI} and P_{ECH} , (b) central electron temperature, T_{e0} , (c) central electron density, n_{e0} , and (d) total radiation power, P_{rad} .

3. Spectral shapes of the tungsten UTAs

Figure 2(a) shows the temporal evolution of the EUV spectrum in the wavelength range of 6–60 Å with a tungsten pellet injection at $t = 4.05$ s. Spectra averaged over (b) 4.15–4.20 s for $T_{e0} = 2.1$ keV, (c) 4.25–4.30 s for $T_{e0} = 3.6$ keV, and (d) 4.65–4.70 s for $T_{e0} = 4.3$ keV are also plotted in Figure 2. When T_{e0} was around 2 keV, W^{24+} – W^{33+} and W^{27+} – W^{29+} UTAs were observed at 20–33 Å and 48–55 Å, respectively. As T_{e0} increased and exceeded 3 keV, the UTA of W^{37+} – W^{42+} appeared at 45–47 Å. As T_{e0} increased further above 4 keV, the W^{37+} – W^{42+} UTA at 45–47 Å was maintained, while the W^{27+} – W^{29+} UTA at 48–55 Å became less intense. These changes in the UTA spectral shape imply a change in the charge state distribution toward the higher charge side, as the electron temperature increases. Figure 3 shows the EUV spectrum in the wavelength range of 130–340 Å, plotted in the same format as Figure 2. When T_{e0} was around 2 keV, UTAs of W^{37+} – W^{42+} at 135–141 Å (the third order of 45–47 Å), W^{27+} – W^{29+} at 144–165 Å (the third order of 48–55 Å), W^{7+} – W^{27+} at 170–210 Å were observed. Unidentified UTAs were also observed at 230–270 Å and 280–320 Å. As T_{e0} increased and exceeded 3 keV, the UTAs were attenuated, except for the UTA of W^{37+} – W^{42+} at 135–141 Å. As T_{e0} increased further above 4 keV, all of the UTAs became weak while several lines of W^{41+} – W^{45+} were maintained.

Acknowledgements

The authors thank all the members of the LHD team for their cooperation with the LHD operation. This work was partially supported by JSPS KAKENHI grant number JP20K03896.

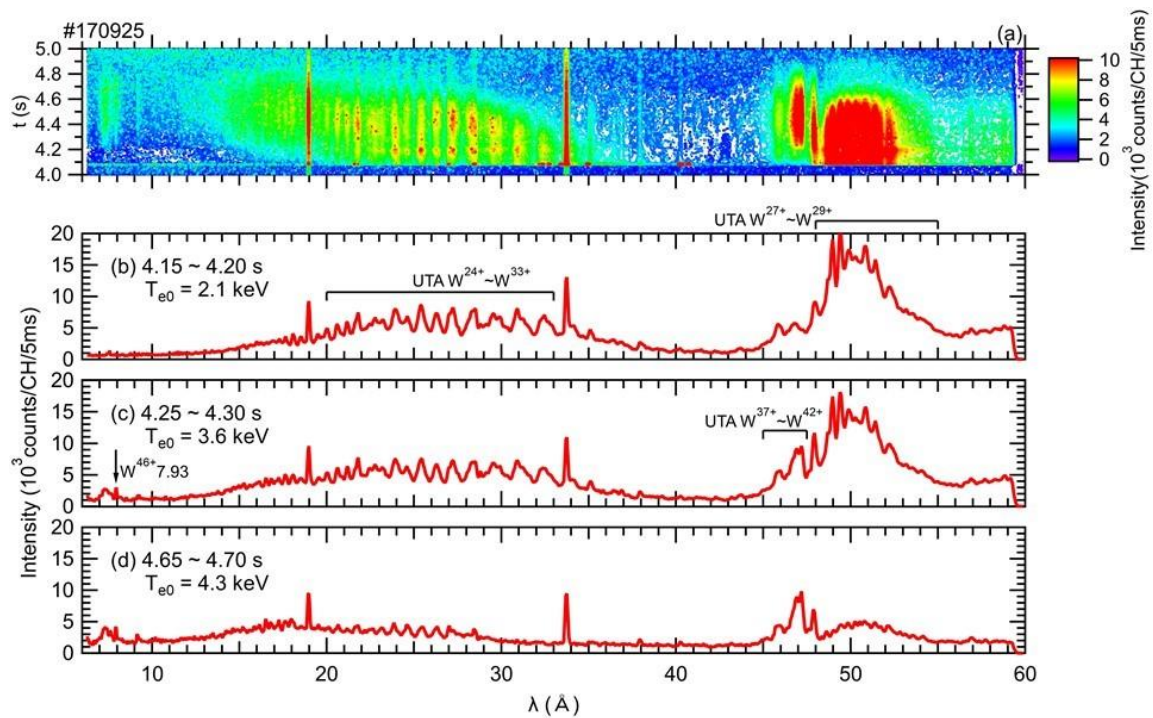


Figure 2. (a) Temporal evolution of the EUV spectrum in the wavelength range of 6–60 Å with a tungsten pellet injection at $t = 4.05$ s. Spectra averaged over (b) 4.15–4.20 s for $T_{e0} = 2.1$ keV, (c) 4.25–4.30 s for $T_{e0} = 3.6$ keV, and (d) 4.65–4.70 s for $T_{e0} = 4.3$ keV, also plotted together.

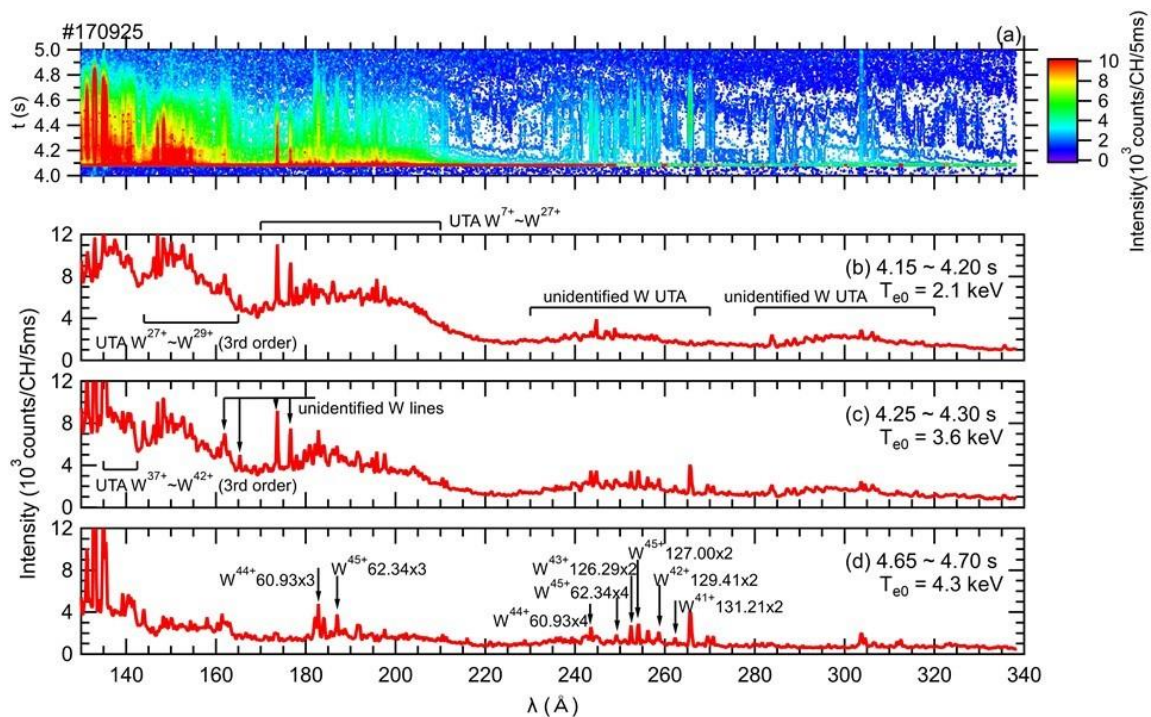


Figure 3. (a) Temporal evolution of the EUV spectrum in the wavelength range of 130–340 Å with a tungsten pellet injection at $t = 4.05$ s. Spectra averaged over (b) 4.15–4.20 s for $T_{e0} = 2.1$ keV, (c) 4.25–4.30 s for $T_{e0} = 3.6$ keV, and (d) 4.65–4.70 s for $T_{e0} = 4.3$ keV, also plotted together.

References

- [1] Pitts R A, Bonnin X, Escourbiac F *et al.*, 2019 *Nucl. Mater. Energy* **20** 100696
- [2] Bauche J and Bauche-Arnoult C 1988 *Phys. Scr.* **37** 659–663
- [3] Takeiri Y, Morisaki T, Osakabe M *et al.* 2017 *Nucl. Fusion* **57** 102023
- [4] Oishi T, Morita S, Kato D *et al.* 2021 *Atoms* **9** 69
- [5] Oishi T, Morita S, Kato D *et al.* 2021 *Phys. Scr.* **96** 025602
- [6] Morita S, Dong C F, Kato D *et al.* 2022 *Springer Proceedings in Physics* **271** 23–36